Letters in Applied NanoBioScience
Open-Access Journal (ISSN: 2284-6808)

Article
Volume 12, Issue 4, 2023, 107
https://doi.org/10.33263/LIANBS124.107

Nano-Encapsulation of Doxorubicin Using Pectin: Safety an Activity on Chemotherapy-Induced Cardiotoxicity in Carcinoma Mice

Neama Mokhtar [1], Fatma Fouda [1], Asmaa Magdy Zaazaa [1,*], Marwa Hanafy Mahmoud [2]

[1] Department of Zoology, Faculty of Women for Arts, Science and Education, Ain Shams University, Cairo, Egypt
[2] Department of Food Technology, National Research Centre, Dokki, Cairo Egypt
* Correspondence: asmaa.zaazaa@women.asu.edu.eg (A.M.Z.);

Scopus Author ID 56948811300
Received: 28.05.2022; Accepted: 21.06.2022; Published: 18.09.2022

Abstract: This study aimed to improve encapsulated doxorubicin ENC-DOX efficiency via loading into pectin nanoparticle PNPs and to investigate the antitumor efficacy of Doxorubicin DOX and ENC-DOX in Ehrlich Ascites Carcinoma EAC bearing-mice. ENC-DOX was optimally fabricated and characterized; female albino mice were divided into 6 groups group 1: control CON, group 2: EAC induced by once injection of 2.5 x 10^6 EAC/ml, group 3: EAC+DOX received 12mg/kg of DOX i.p, group 4: EAC+PNPs received orally 12mg/kg PNPs, group 5: EAC+DOX+PNPs as the same previous dose and route, and group 6: EAC+ENC-DOX received 12mg/kg of ENC-DOX orally. The treatment with ENC-DOX resulted in a significant reduction in mean tumor weight MTW, improvement in mean survival time MST, and an increase in life span ILS. Also, ENC-DOX ameliorated the cardiac CK and LDH and decreased MDA levels associated with improvement in GPX, GSH, and SOD levels and reduced the level of TNF-α and MCP-1; also, ENC-DOX caused depletion in caspase-3 and P53 with an elevation of Bcl2 level comparing with treatment with free DOX, dimensioned histological lesions were noticed in the heart tissue sections of mice administrated ENC-DOX. The treatment of EAC mice with ENC-DOX displayed a promising potential antitumor effect with greater safety than free DOX.

Keywords: cardiotoxicity; drug delivery system; pectin nanoparticles; Doxorubicin.

© 2022 by the authors. This article is an open-access article distributed under the terms and conditions of the Creative Commons Attribution (CC BY) license (https://creativecommons.org/licenses/by/4.0/).

1. Introduction

One of the leading causes of global morbidity and mortality is cancer [1]. Ehrlich ascites carcinoma (EAC) is one of the most prevalent Experimental cancers with important modeling implications [2]. Chemotherapeutic medicines are frequently employed to eliminate tumor cells, but they all have side effects because they harm healthy cells [3]. Doxorubicin (DOX) is an anthracycline antibiotic used to treat a variety of cancers for decades. Most organs, particularly the heart, are poisonous to DOX [4]. The heart has low antioxidant levels compared to other organs, which contributes to its high tolerance to chemotherapy-induced damage [5]. DOX causes cardiotoxicity by producing free radicals and reactive oxygen species, incrementing oxidative stress and depleting the antioxidant system, triggering apoptosis and causing DNA damage [6].

Nanoparticles have opened up new possibilities for chemotherapy. Targeted drug delivery to the tumor location or a specific group of cells using ingeniously made nanoparticles almost eliminates side effects in normal tissues and organs [7]. Chemical stability, selectivity,

sustained drug release, enhanced drug solubility, and lower toxicity are all properties of the suitable nanocarriers that have been studied extensively for targeted drug delivery systems [8]. Natural polymers have been utilized for nanoencapsulation as carriers of drugs because they have key functional groups that can be conjugated to the drugs. Furthermore, polymers can aggregate to produce cross-links that can hold and encapsulate the drug with a hydrophilic surface [9].

Pectin is an anionic polysaccharide polymer present in the cell wall of fruits and plants [10]. Pectin-based nanomaterials are suitable for encapsulation due to their properties like Good water solubility, high surface area, biodegradability, cytocompatibility, extended drug half-life, and controlled drug release. When compared to bulk pectin, pectin nanoparticles have a specific surface area [11]. The present work was designed to evaluate the antitumor activity and safety of ENC-DOX compared to the commercially used drug DOX in Ehrlich Solid Carcinoma-bearing mice.

2. Materials and Methods

2.1. Drugs and chemicals.

Doxorubicin was obtained from Sigma-Aldrich (St. Louis, USA). Pectin was extracted from orange peel. All chemicals and reagents of pectin extraction, Nano pectin preparation, and doxorubicin encapsulation, including folic acid, fish oil, citric acid, ethyl alcohol, hydrochloric acid, sodium nitrate, and sodium azide, were of analytical grade and were gotten from Sigma-Aldrich (St. Louis, USA).

2.1.1. Pectin extraction.

Orange peel was obtained after juice extraction, and then it was dried at 40^{o}C for 13 hr. and milled according to Mohammed *et al*. [12]. Pectin was extracted, Step 1 extraction: Orange peel powder 100 g was mixed with 2000 mL of distilled water until stirring. The pH was adjusted to 1.9 using mineral acid HCl with continuous stirring for about 10 min. This mixture was boiled for 1 hr. Then it was dried at 40°C and kept at 4°C until further analysis. Step 2 extraction and purification: All slurries were centrifuged at 4000 rpm for 30 min (4 ^{o}C). For the precipitation of pectin, a 1:2 V/V ratio of ethanol was added and kept to stand for about 2hrs at room temperature, then centrifuged at 4000 rpm/20 min/ 4^{o}C. The precipitated pectin was collected and dried at 4^{o}C.

2.1.2. Nano pectin preparation.

Pectin (25g) was mixed with 1 L of Distilled water, then treated with a microwave oven (Samsung, Model MF245, Korea) at a power of 945 W for 30 min. A high-speed homogenizer blended it at 20000 rpm for 30 min (CAT, Unidrive 1000 D, M.Zipperer GmbH, Germany) followed by prop-ultrasonic (SONICS, Vibra-cell, VCX750, USA). In a lab spray dryer (Model SP1500, Fanyuan Instrument Co., Shanghai, China) fitted with a pressure air atomizing nozzle at 2.5 bar air pressure, an inlet air temperature of 180 5 °C, an outlet air temperature of 90 5 °C, and a feed flow rate of 450 mL/h, the material was then spray dried to format powders. Before the further examination, the dry powder was gathered and kept in an airtight, dark bottle at 4°C.

2.1.3. Nano formulation of Doxorubicin.

The formula of nanoemulsion of folic acid and Doxorubicin was prepared in two separate nano-capsulessurrounded by microcapsule.

2.1.3.1. Water oil (W/O) nanoemulsion.

According to Assadpour & Jafari [13], with a few adjustments, water oil nanoemulsion was made by spontaneous emulsification. Briefly, the aqueous phase was prepared by mixing (folic acid or Doxorubicin) each in a separate solution with Span 80 using a magnetic stirrer (VELP, Germany) at 500 rpm and then added drop-wise to the fish oil phase while magnetically stirring at 1500 rpm. The formulation was composed of oil and surfactant solution.

2.1.3.2. Biopolymer solution preparation.

To get 100 g of solutions, 2.5 g of pectin powder was dissolved in boiling deionized water. Whey protein concentrate (WPC) aqueous solutions were also made simultaneously by blending 10g of WPC powder with 45 ml of deionized water. Solution solutions were gently swirled on a magnetic stirrer for at least 30 minutes. To fully hydrate the biopolymers, pectin and WPC solutions were combined and left at room temperature overnight. 75 ml of the maltodextrin solution were added last.

2.1.3.3. Water oil water (W/O/W) nanoemulsion.

It was blended with the W/O emulsion and biopolymer solution in a high-speed homogenizer (CAT, Unidrive 1000 D, M. Zipperer GmbH, Germany) at a speed of 20,000 revolutions per minute (SONICS, Vibra-cell, VCX750, USA). Spray drying of emulsions (encapsulation of Doxorubicin): According to Mohammed *et al*. [14], a spray dryer (B-290, Buchi) outfitted with a pressure air atomizing nozzle at 2.5 bar air pressure, inlet air temperature of 180±5 °C, and outlet air temperature of 90±5 °C with a feed flow rate of 450 ml/h transformed the prepared emulsion solutions into encapsulated powder. Before the further examination, the dry powder was gathered and kept in an airtight, dark bottle at 4°C.

2.1.4. Scanning electron microscopy (SEM) of pectin powders.

A small layer of gold was applied after the pectin powder was scattered onto a two-sided adhesive tape. The morphological characteristics of the particles were examined using a field emission scanning electron microscope (S- 4160 Cold Field-Emission SEM, QUANTA, FEG 250, Thermo Fisher Scientific, USA) with an augmented voltage of 320 kV and captured on camera at 6000.

2.1.5. Zeta potential.

Using a dynamic light scattering technique, the Zeta potential of pectin granules was examined (Zeta-sizer Nano Zs, Malvern Instrument, Malvern, UK). To prevent double scattering, all materials were diluted in water to the final concentration of 0.01 grams per 100 ml of pure water. A Zeiss optical microscope (Germany) was used for microstructure analysis, and image software was used to analyze the obtained images [15].

2.2. Animals.

Ehrlich ascites carcinoma cells grew faster and had a total cell count in female mice than in male mice [16]. So, the current study used female mice that were obtained from the National Institute of Cancer, University of Cairo.

A total number of 305 adult female Swiss albino mice weighing 25-30 gm were obtained from the animal house of Theodore Bilharis Institute (Cairo). Mice were housed in plastic cages at room temperature and under natural lighting conditions. Animals were fed a regular pellet diet with tap water. Animals were exposed to pre-experimental acclimation for two weeks until starting the experiment. All animals were cared for according to the instructions for animal experiments authorized by the ethical committee, faculty of science, Ain Shams University, Cairo, Egypt.

2.2.1. Tumor cell line.

Ehrlich Ascites Carcinoma cells (EAC) were supplied from the pharmacology and experimental oncology unit of the National Cancer Institute (NCI), Cairo University, Egypt. EAC cells can grow in both solid and ascites forms. The tumor line was maintained in ascites form in female mice by weekly intraperitoneal injection (i.p.) of $2.5x10^6$ tumor cells/mouse into the peritoneal cavity of the mice and allowed to multiply according to the method commended by the Egyptian National Institute of Cancer, Cairo University [16]. The ascites fluid containing EAC cells developed within 10 days and was thinly collected by i.p. puncture using a sterile syringe followed by dilution and counting of the cells. Cells were counted before injection using Neubauer Haemocytometer, and dilutions were made with physiological saline. A model of the solid tumor was induced in female mice by injecting 0.2 ml viable ($2.5x10^6$ cells per mouse) EAC cells subcutaneously (S.C.) into the back of each mouse and lifted for 10 days [17].

2.2.2. Cell viability

Ascites fluid was collected on the seventh day after EAC inoculation and submitted to a trypan blue dye exclusion technique for cell viability determination [18]. Under a microscope, the number of live cells (unstained) was calculated, and the average from five squares was taken. The cells which took trypan blue-taking cells were declared non-viable Figure 1. The concentration of viable cells (expressed as follows: C= T x D x 104), where C= concentration of viable cells/ml, T= Average no. of viable cells per square, and D= dilution factor.

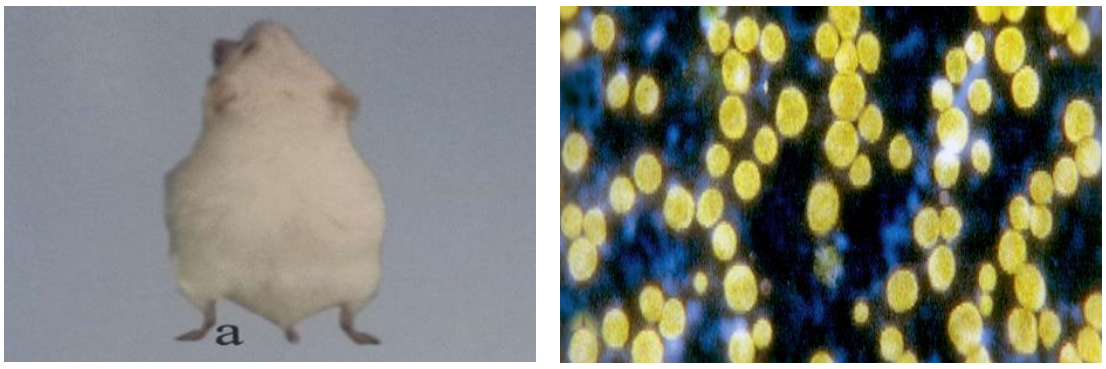

(a) **(b)**

Figure 1. (a) shows the culture of EAC in vivo (in the abdominal cavity of the female mouse). (b) Showing the normal EAC cells X200.

2.2.3. Ehrlich solid carcinoma induction.

Ehrlich Ascites Carcinoma (EAC) cells obtained from the ascitic fluid of EAC-bearing female mice were injected into forty female mice to form Ehrlich Solid Carcinoma (ESC). Intramuscularly in the left thigh of each mouse, about 2.5×10^6 viable EAC cells present in 0.2 ml of diluted ascitic fluid (1:10) with saline were injected on day zero [19].

2.3. Experimental design.

2.3.1. Antitumor studies.

The antitumor activities of DOX and/or ENC-DOX were evaluated on 215 mice bearing solid Ehrlich Carcinoma that were divided into two main groups, 40 mice were used to determine the mortality rate in the first group and subdivided into five groups (n=8) as flow: Gr.1: (EAC) group, EAC cells (2.5×10^6 viable EAC) was inoculated intramuscularly in the left thigh of each female mouse to induce solid tumors. Gr.2: (EAC+DOX) group, after Ten days from the inoculation of EAC cells, the animals were treated with DOX (12mg/kg, i.p.) three days a week for three weeks Gr.3: (EAC+PNPs) group, after Ten days from the inoculation of EAC cells, the animals were treated orally with pectin nanoparticles (12mg/kg) three days a week for three weeks.Gr4: (EAC+DOX+PNPs) group, after Ten days from the inoculation of EAC cells, the animals were treated with DOX and pectin nanoparticles at the same previous corresponding dose, period, and route of administration. Gr5: (EAC+ENC-DOX) group, after Ten days from the inoculation of EAC cells, the animals were orally treated with encapsulated doxorubicin (12mg/kg) three days a week for three weeks [20,21].

In the other group, 175 mice were used to evaluate the mean tumor weight (MTW). Mice of this group were left until the study was finished and were divided into five groups (n=35) equal in size as flow: Gr1: EAC group, Gr2: EAC+DOX group, Gr3: EAC+PNPs, Gr4: EAC+DOX+PNPs, Gr5: EAC+ENC-DOX (mice of these groups were treated as declared previously). After that, the mice in this group were left untreated until the study was finished. Every week, three animals were killed to measure the control mean tumor weight (MTWc) and test mean tumor weight (MTWt). The control mean survival time (MSTc), the test mean survival time (MSTt), the increase in life span (ILS, %) and the inhibition ratio of tumor growth (T/C %) were evaluated according to Fahim *et al*. [22], where: the days in which animals were only alive is considered the MST.

$$ILS\% = \frac{MSTt}{MSTc} \times 100$$

$$(T/C\%) = \frac{MSTc - MTWt}{MSTc} \times 100$$

2.3.2. Biochemical and histopathological studies.

90 animals were branched into six groups, 15 mice in each group as follows: Gr.1: control (CON) group mice injected i. p. with physiological saline, Gr2: EAC group, Gr3: EAC+DOX, Gr4: EAC+PNPs, Gr5: EAC+DOX+PNPs and Gr6: EAC+ENC-DOX (from Gr2-Gr5, mice were treated as declared previously).

2.3.3. Blood sampling.

At the end of the experimental period (32 days), mice were sacrificed under ether anthesis; blood samples were collected in a dry clean centrifuge tube and kept for 15 minutes, then centrifuged at 3000 rpm for 15 minutes. The sera were collected in Eppendorf tubes. Solid tumors were separated from each mouse, washed with distilled water, and weighed. The heart was dissected, washed, weighed, and fixed in 10 % neutral buffered formalin (PH 7.4) for histopathological investigation. Each heart was separated into two parts. One of them was rapidly homogenized to give 10% (w/v) homogenate in a medium of ice with phosphate buffer (pH: 7.4). The homogenate was centrifuged at 1800 ×g for 10 min at 4°C. The supernatant (10%) was separated and stored at −20 °C for biochemical determinations. The second part of the heart was fixed in 10% formalin saline for histopathological investigation.

2.3.4. Assessment of oxidative stress.

The following parameters were used to assess oxidative stress: the level of cardiac MDA was evaluated calorimetrically as reported by Ohkawa *et al*. [23] using the kit from Biodiagnostic Company (Giza, Egypt). The activity of Cardiac superoxide dismutase SOD was evaluated colorimetrically, as stated by Nishikimi *et al*. [24], using the Biodiagnostic Company (Giza, Egypt) kit. A spectrophotometer operated the level of reduced glutathione (GSH) in the heart tissue in accordance with Beutler *et al*. [25] using the kit from Biodiagnostic Company (Giza, Egypt). Cardiac Glutathione peroxidase (GPX) was evaluated colorimetrically using the kit of (Bio-diagnostic, Egypt), as reported by Paglia and Valentine [26].

2.3.5. Determination of inflammatory markers.

Quantitative hepatic tumor necrosis factor-alpha (TNF-α) was determined using TNF-α ELISA kit (Abbexa Ltd., Cambridge Science Park, Cambridge, CB4 0EY, UK), succeeding the manufacturer's guidelines. Monocyte chemoattractant protein-1 (MCP-1) of heart was carried out according to the instructions of manufacturing and guidelines of (Cloud Clone Corp, USA) using Rat MCP-1 ELISA kit.

2.3.6. Estimation of apoptotic and anti-apoptotic markers.

Quantitative determination of cardiac Caspase-3 was carried out according to the instructions of manufacturing and guidelines of (Cloud Clone Corp, USA) using Rat CASP3 ELISA Kit. Tumor Protein (p53) was determined according to the instructions of manufacturing and guidelines (Cloud-Clone Corp, USA) using the P53 Rat ELISA kit. Quantitative B-Cell Leukemia/Lymphoma 2 (Bcl2) was determined using a Rat BCL2 ELISA kit (Cloud-Clone Corp, USA).

2.3.7. Biochemical determinations.

Creatine kinase level of (CK) was determined according to manufacturer instructions and guidelines of (Bio-vision, USA)) using Rat CK ELISA Kit. Cardiac lactate dehydrogenase (LDH) was determined according to manufacturer instructions and guidelines of (CUSABIO Technology LLC, Houston, Texas) using Rat LDH ELISA Kit.

2.3.8. Histopathological investigation.

Autopsy samples were taken from the heart and fixed in 10% neutral buffered formalin. Tap water was used for washing, and dehydration was carried out using serial dilutions of alcohol (methyl, ethyl, and absolute ethyl). The clearance of the Specimens was made by xylene, and then the specimen was embedded in paraffin at 56 degrees for twenty-four hours in a hot air oven. Sectioning was operated using Paraplast wax tissue blocks by rotatory microtome at a thickness of 4 microns. The prepared sections of the heart tissue were plotted on glass slides, deparaffinized, and hematoxylin & eosin were used for staining [27].

2.4. Statistical analysis.

In this study, all results existed as mean±standard error of the mean. To compare the significance between every two groups, Statistical Package for the Social Sciences program, version 19.0, was used. The difference was considered statistically significant at $p<0.05$. The difference in Percentage is the percent of dissimilarity for the corresponding control group and carried out according to the consequent rule:

$$\%Difference = \frac{treated\ value - control\ value}{control\ value} \times 100$$

3. Results and Discussion

3.1. Characterization of formulated nanoparticles.

3.1.1. Nano-pectin.

The Scanning electron microscopy (SEM) photomicrograph of treated pectin samples showed a smooth and complete surface Figure 3 compared to pectin without treatments Figure 2. The pectin was treated with a spray dryer; the particles were seen near spherical when viewed through an electron microscope. The micrograph of untreated pectin revealed that all pectin surfaces had an uneven surface Figure 2. PNPs had a size of 805.4 nm and zeta potential (–52.1 mV).

3.1.2. Nano-Encapsulated Doxorubicin.

The SEM of the encapsulated Doxorubicin showed the microstructures of nano-doxorubicin/folic acid wrapped in a pectin layer Figure 4.

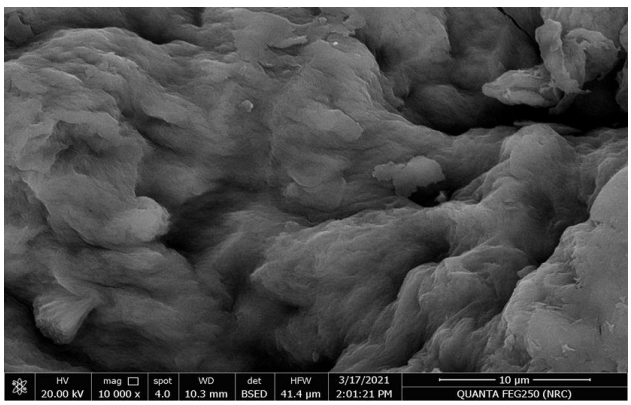

Figure 2. SEM image of untreated pectin showing uneven surfaces.

WPC nanoparticles made up the encapsulated powder in the size range of 200–500 nm. The oil layer around these particles was covered by another layer of pectin, resulting in a larger particle range (2000–9000 nm). Nano doxorubicin capsule powder had a narrow distribution and a tiny diameter of 263 nm. The zeta potential result demonstrated that the powder of nano-doxorubicin particles had a negative charge (-50 mV).

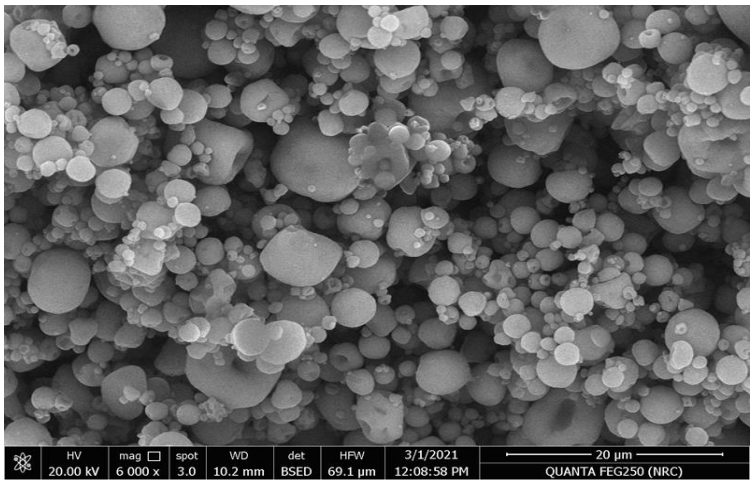

Figure 3. It shows SEM image showing Particles of nano-pectin with the size of 805.4 nm.

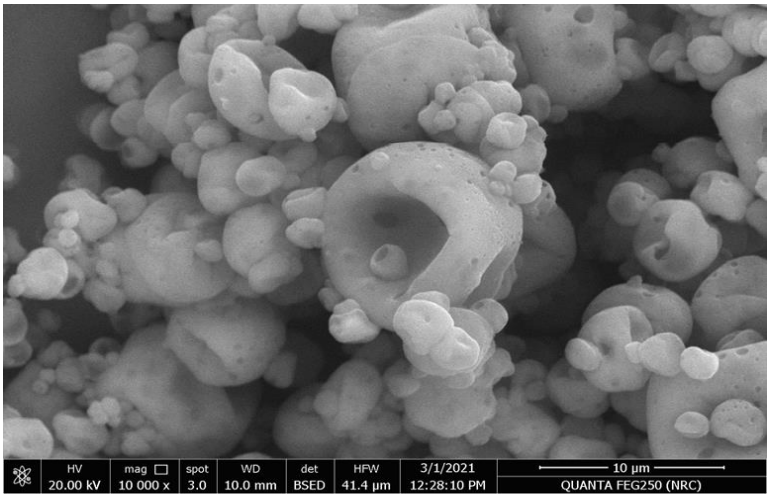

Figure 4. It shows SEM image of the doxorubicin nanocapsule showing particle size range from (2000–9000 nm) nanometer.

3.2. The antitumor studies.

The treatment of EAC mice with the DOX+PNPs and ENC-DOX resulted in an increase in the life span (ILS %), which reached to123.33%, and 154.44%, respectively (table 1), compared to the EAC mice treated with DOX-free (115.55%). The EAC group treated with PNPs showed no remarkable distinction in the mean tumor weight (MTW) (4.4g) compared with EAC group (4.98g), while high retardation was noticed in the mean tumor weight in the groups treated with DOX+PNPs and ENC-DOX (3.18g) and (2.99g), respectively. On the other hand, the ENC-DOX group revealed the most elevation of the tumor growth inhibition ratio (T/C %) (39.95%) as compared with the treatment of EAC mice with free DOX (29.31%).

Table 1. The antitumor activities of DOX or/and ENC-DOX solid Ehrlich carcinoma mice.

PTI	Gr. (EAC)		Gr. (EAC+DOX)		Gr. (EAC+PNPs)		Gr. (EAC+DOX+PNPs)		Gr. (EAC+ENC-DOX)	
(Days)	M	MTW±SE	M	MTW±SE	M	MTW±SE	M	MTW±SE	M	MTW±SE
10	0/8	1.21±0.09	0/8	1.13±0.07	0/8	1.16±0.08	0/8	1.23±0.05	0/8	1.08±0.02
17	0/8	2.41±0.32	0/8	1.83±0.44	0/8	2.81±0.21	0/8	1.42±0.09	0/8	1.21±0.06
24	0/8	3.01±0.26	0/8	2.41±0.53	0/8	3.42±0.29	0/8	1.74±0.09	0/8	1.42±0.05
31	0/8	4.81±0.31	0/8	2.83±0.42	0/8	4.26±0.38	0/8	2.22±0.12	0/8	1.78±0.08
38	1/8	5.61±0.87	0/8	3.41±0.54	3/8	4.92±0.28	0/8	2.63±0.23	0/8	2.31±0.11
45	2/8	6.72±0.91	2/8	3.72±0.60	4/8	5.55±0.40	2/8	3.12±0.11	0/8	2.84±0.14
52	5/8	7.22±0.85	5/8	4.26±0.81	6/8	6.32±0.22	4/8	3.98±0.26	0/8	3.33±0.19
59	8/8	8.04±0.87	6/8	5.21±0.79	8/8	6.78±0.30	5/8	4.45±0.31	1/8	3.92±0.21
66			8/8	6.88±0.91			6/8	5.09±0.44	2/8	4.02±0.17
73							8/8	5.92±0.39	4/8	4.43±0.22
80									5/8	4.63±0.23
87									8/8	5.02±0.36
MTW	4.98		3.52		4.4		3.18		2.99	
MST (days)	45		52		45		55.5		69.5	
ILS%	-		115.55		100		123.33		154.44	
T/C%	-		29.31		11.64		36.14		39.95	

T/C= Tumor inhibition ratio. ILS= Increase of life span. MST (days) = Mean survival time. MTW= Mean tumor weight. M= Mortality. PTI= Post tumor inoculation.*3.3. Effect of treatment with PNPs, DOX+PNPs, and ENC-DOX on cardiac oxidative stress marker MDA and antioxidant markers SOD, GSH, and GPX.*

3.3. Effect of treatment with PNPs, DOX+PNPs, and ENC-DOX on cardiac oxidative stress marker MDA and antioxidant markers SOD, GSH, and GPX.

The data in Table 2 revealed marked oxidative stress represented by significant elevation (P<0.05) of MDA level and reduction in SOD, GPX, and GSH levels of the EAC group's heart tissue as compared to the CON group. MDA level recorded a significant increase while SOD, GPX, and GSH recorded a depletion (P<0.05) in DOX group as compared to EAC group. The value of MDA decreased to highly significant, and the values of SOD, GPX, and GSH increased in PNPs, DOX+PNPs, and ENC-DOX group as compared to DOX group.

Table 2. Effect of treatment with PNPs, DOX+PNPs, and ENC-DOX on MDA, SOD, GPX, and GSH of EAC-bearing mice.

Parameter / group	MDA (nmol/g.tissue)	SOD (U/g.tissue)	GSH (mmol/g.tissue)	GPX (U/g.tissue)
CON	6.32±.0.92	105.33±10.61	20.41±2.52	.706±.01
EAC	35.64±3.21 [a] a (463.91%)	40.25±5.42[a] a (-14.32%)	5.04±0.62[a] a (-75.31%)	0.013±.003[a] a (-98.61%)
EAC+DOX	33.42±4.35[b] b (-6.28%)	29.63±3.14[b] b (-26.83%)	7.52±0.81[b] b (49.26%)	0.009±.002[b] b (576.41%)
EAC+PNPs	15.22±2.31[c] c (-54.45%)	55.82±6.26[c] c (98.34%)	9.72±1.40[c] c (29.25%)	0.155±.012[c] c (68.91%)
EAC+DOX+PNPs	19.42±2.12[c] c (-41.84%)	35.22±4.12[c] c (18.83%)	11.25±1.26[c] c (49.64%)	0.151±.009[c] c (64.78%)
EAC+ENC-DOX	10.26±1.14[c] c (-69.29%)	85.33±6.22[c] c (187.89%)	15.33±2.13[c] c (103.85%)	0.392±.004[c] c (326%)

a: statistically significant at P<0.05 vs. the control group (CON). b: statistically significant at P<0.05 vs. EAC group. c: statistically significant at P<0.05 vs. DOX group.

3.4. Effect of treatment with PNPs, DOX+PNPs, and ENC-DOX on pro-inflammatory markers (MCP-1) and (TNF-α).

The data levels of MCP-1 and TNF-αof heart were recorded in table 3. MCP-1 and TNF-αof heart revealed a significant increase in EAC group as compared to CON group (P<0.05), also MCP-1 and TNF-α recorded a low significant increase in DOX treated group compared with EAC group (P<0.05). However, PNPs, DOX+PNPs, and ENC-DOX recorded

a significant decline (P<0.05) in levels MCP-1 and TNF-α of the heart compared to its level in the DOX group.

Table 3. Effect of treatment with PNPs, DOX+PNPs, and ENC-DOX on MCP-1 and TNF-α of EAC bearing mice.

Parameter / group	MCP-1 (ng/ml)	TNF-α (pg/g tissue)
CON	1.92±.04	84.22±6.72
EAC	15.81±.34[a] a (732,1%)	352.79±12.26[a] a (318.8%)
EAC+DOX	19.73±.29[b] b (24.79%)	398.64±16.71[b] b (10.44%)
EAC+PNPs	11.36±.25[c] c (-42,42%)	288.41±11.78[c] c (-27%)
EAC+DOX+PNPs	13.96±.21[c] c (29.24%)	187.78±10.32[c] c (-52.89%)
EAC+ENC-DOX	5.65±.1[c] c (-71.36%)	105.11±9.23[c] c (-73.6%)

a: statistically significant at P<0.05 vs. the control group (CON). b: statistically significant at P<0.05 vs. EAC group. c: statistically significant at P<0.05 vs. DOX group.

3.5. Effect of treatment with PNPs, DOX+PNPs, and ENC-DOX on cardiac pro-apoptotic marker caspase-3 and tumor protein P[53] and anti-apoptotic marker BCL2.

The data levels of Caspase-3, P[53,] and BCL2 of the heart were recorded in table 4. Cardiac caspase-3 and P[53] revealed a significant increase, while BCL2 was reduced in EAC group as compared to CON group (P<0.05). Also, caspase-3 and P[53] recorded a low significant increase with reduction of BCL2 in DOX treated group compared with EAC group (P<0.05). However, PNPs, DOX+PNPs, and ENC-DOX recorded a significant decline (P<0.05) in caspase-3 and P[53] levels and elevation in BCL2 of liver tissue compared to DOX group.

Table 4. Effect of treatment with PNPs, DOX+PNPs, and ENC-DOX on caspase-3, p[53], and Bcl2of EAC bearing mice.

Parameter / group	Caspase-3 (ng/g. tissue)	P53 (pg/g, tissue)	Bcl2 (pg/g, tissue)
CON	10.16±1.31	71.51±.39	86.78±1.39
EAC	65.23±7.14[a] a (542.02%)	188.45±1.51[a] a (63.54%)	10.72±.57[a] a (-87.64%)
EAC+DOX	76.26±6.34[b] b (16.9%)	200.33±1.1[b] b (6.12%)	8.32±.24[b] b (-22.38%)
EAC+PNPs	53.62±5.29[c] c (-29.68%)	169.58±.34[c] c (-15.2%)	27,43±.49[c] c (229.68%)
EAC+DOX+PNPs	49.25±5.33[c] c (-35.41%)	177.86±.55[c] c (-11%)	21.37±.31[c] c (156.85%)
EAC+ENC-DOX	19.73±2.03[c] c (-79%)	152.74±1409.37[c] c (-33.34%)	61.25±.85[c] c (636.17%)

a: statistically significant at P<0.05 vs. the control group (CON). b: statistically significant at P<0.05 vs. EAC group. c: statistically significant at P<0.05 vs. DOX group.

3.6. Effect of treatment with PNPs, DOX+PNPs, and ENC-DOX on heart CK and LDH levels in EAC mice.

Data recorded for heart CK and LDH are presented in table 5. Heart CK and LDH levels recorded a significant elevation (P<0.05) in EAC group as compared to CON group; moreover, they recorded a significant depletion In DOX group (P<0.05) as compared to EAC group. CK and LDH levels in heart tissue recorded a significant decrease (P<0.05) in PNPs, DOX+PNPs, and ENC-DOX as compared to DOX group.

Table 5. Effect of treatment with PNPs, DOX+PNPs, and ENC-DOX on CK and LDH of EAC bearing mice.

Parameter / group	CK (pg/ml)	LDH (mu/ml)
CON	133.3±1.5	223.69±1.5
EAC	322.65±2.12[a] a (142.62%)	492.37±1.6[a] a (120.21%)
EAC+DOX	258.14±1.73[b] b (-19.91%)	418.91±2.1[b] b (-14.92%)
EAC+PNP	207.02±12.28[c] c (-19.83%)	378.94±4.47[c] c (-9.54%)
EAC+DOX+PNP	201.71±.66[c] c (-21.81%)	354.41±1.09[c] c (-15.39%)
EAC+ENC-DOX	175.58±84[c] c (-31.62%)	287.08±1.23[c] c (-31.48%)

a: statistically significant at P<0.05 vs. the control group (CON). b: statistically significant at P<0.05 vs. EAC group. c: statistically significant at P<0.05 vs. DOX group.

3.7. Histopathological investigation.

Histopathological investigations of the heart of EAC group showed myocarditis manifested by intense mononuclear inflammatory cells infiltration between the muscle fibers. The muscle fibers suffered from vacuolar degeneration and necrosis. Pericarditis was noticed in some of the examined sections. The blood vessels within the myocardium were severely congested Figure 5B. Moreover, the EAC+DOX group showed mild degenerative changes in the myocardium (Figure 5C). The heart of the EAC+PNPs group exhibited focal aggregations of mononuclear inflammatory cells with necrosis of some myocardial fibers (Figure 5D). Sections from EAC+DOX+PNPs revealed mild mononuclear inflammatory cells in some instances (Figure 5E). The group that received ENC-DOX appeared normal and free from any detectable histological alterations (Figure 5F).

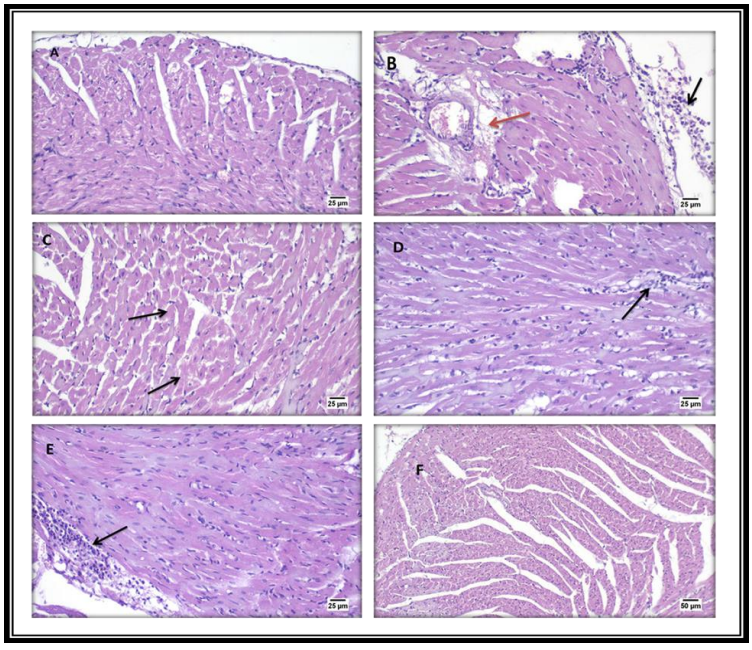

Figure 5. Photomicrographs of H and E stained heart sections of CON, EAC, DOX, PNPs, DOX+ PNPs, and ENC-DOX groups. (A) Photomicrograph of heart section of CON group showing normal myocardium. (B) Photomicrograph of the heart of EAC group showing pericarditis (black arrow) with mononuclear inflammatory cells infiltration in the myocardium; note the perivascular edema (red arrow). (C) Section of the heart of EAC+DOX group showing the degeneration of muscle fibers (black arrows). (D) Cardiac section of EAC+PNPs group showing focal mononuclear inflammatory cells aggregation (black arrow). (E) Cardiac section of EAC+DOX+PNPs group showing normal myocardium with focal mononuclear inflammatory cells infiltration (black arrow). (F) The heart section of the group treated with EAC+ENC-DOX showed normal myocardium.

3.8. Discussion.

The emulsion is the upcoming promising encapsulation and delivery technology for either bioactive compounds or drugs. They have great advantages, such as controlled release and chemical stability [28,29]. Our study aimed to coordinate a W/O/W double emulsion by having the oil molecules surrounding Doxorubicin and folic acid wrapped in a WPC membrane. Then all the molecules were contained within another layer of pectin to produce a large molecule that collects the small molecules inside. Those structures allow more ingredient protection [30] and the protection of all body organs, forming doxorubicin hazards.

The results of SEM of treated pectin samples showed smooth and complete surface ed to pectin without treatments with uneven surfaces. The pectin was treated with a spray dryer, and the particles were seen to be near-spherical, and this shape is essential for the food industry [31].This is important because a more uniform spherical shape has been confirmed to correspond to reduced gas permeability and improved material retention and protection. On the other side, other treated pectin has a more compact, multi-laminate, and flaks surface that seems hard. Moreover, the microstructures of nano-doxorubicin/folic acid wrapped in a pectin layer were illustrated by SEM to establish the shapes and sizes. The surface pores of capsules were visible in the SEM microstructure. This structure allowed for high release, which was anticipated due to the capsule's increased surface air permeability and high solubility [32,33].

The size and distribution of particles may have a significant role in deciding the fate of capsules after oral delivery. The nano-pectin and nanocapsule size and distribution were measured using the dynamic light scattering (DLS) method, which is the best technique for assessing the size distribution profile of suspended in solution [34]. Different particle sizes can change the physicochemical properties of powders, whereas; smaller and finer particles in capsulated powders can help increase dispersibility and solubility. Typically, achieving good stability requires a minimum zeta potential of 30 mV for nanosuspensions to be electrostatically stabilized. Furthermore, 20 mV of zeta potential is sufficient in the case of the combination of electrostatic and steric forces. This is because the hydrophilic surfactant coat can improve the stability of the emulsion by further hydrating the surface layer [35].

The zeta potential of treated pectin samples has a great negative charge – 52.1. This indicates that the nano-pectin sample showed higher stability in aqueous dispersion. This result was agreed with Guo *et al*. [36], who clear that polysaccharides, such as pectin and soluble soybean polysaccharides (SSPs) with zeta potentials between (30 > zeta potential >-30 mV) be a tendency to coagulate or flocculate and hard to have a stable colloidal or emulsion system only at the electrokinetic potential. The zeta potential result demonstrated that the powder of nano-DOX particles had a negative charge (-50 mV) and could be considered with great solubility and stability. This indicates that the DOX-loaded polymer system was assumed to be a stable system. Because of the trapping of polymer molecules, the DOX-loaded polymer capsules had a large surface area, which could explain why the negative charge on the capsules' surfaces was enhanced.

The current study revealed retardation of the solid tumor burden in tumor-bearing mice treated with DOX plus PNPs also enhanced the survival time of EAC-bearing mice as compared to the treatment with DOX alone. Moreover, the treatment with ENC-DOX exerted a more marked effect, represented by higher increases in the tumor inhibition ratio and the life span of animals. The present findings revealed that ENC-DOX exerted antitumor activity through the inhibition of tumor proliferation and interference with the metabolism of the cells.

Our finding is in agreement with Lara-Espinoza *et al*. [37], who reported that galectin-3 (Gal-3), (a β-galactoside-binding protein) overexpressed in various types of tumor, plays a key role in cancer development and progression including tumor cell growth, adhesion, and metastasis. Galectin-3 is an adhesive molecule that can bind specifically to the pectin molecule's β-galactose units, making pectin a tumor-targeting agent [38]. In addition, Sayed *et al*. [39] reported that metastatic cells could be destroyed through the inhibition of Gal-3. On the other hand, Matarrese *et al*. [40] reported that the overexpression of Gal-3 can trigger cell cycle arrest at the growth 1 (G1) phase and influence mitochondrial homeostasis. Also, some glycoproteins in the epithelial membrane can be recognized and endocytosed by Gal-3 [41].

The results of our study also revealed that the administration of ENC-DOX resulted in a significant elevation in the mean survival time and reduction in MTW of tumor-bearing mice compared with the treatment with free DOX. Our result follows Zhang *et al*. [42], who stated that the nanometric size of pectin nanoparticles enables them to easily enter the tumors, which makes pectin nanoparticles more accessible carriers for anticancer drugs. Also, Pectin nanoparticles can induce apoptosis in cancerous cells [43]

Data presented in the current study demonstrated that there is a significant increase in cardiac oxidative stress marker MDA in tumor-bearing mice with a significant reduction in SOD, GPX, and GSH in EAC-bearing mice versus to normal control group; they may be due to the development of primary and secondary carcinoma [44]. Moreover, our results agree with Forman *et al*. [45], who stated that oxidative stress resulting from the excessive accumulation of reactive oxygen species plays a key role in cancer development.

Mice administrated DOX showed a significant increase in cardiac MDA level correlated with a significant decrease in SOD and GPX activity as well as GSH level as compared to EAC group. Our findings demonstrated the occurrence of oxidative stress in doxorubicin-injected mice, which may be due to the increase of reactive oxygen species (ROS) production by DOX [46]. Higher production of free radicals results in oxidative stress, which leads to the increment of MDA synthesis due to lipid peroxidation and macromolecule damage such as lipids [47]. Our results are consistent with Yu *et al*. [48], who concluded that Doxorubicin reduces enzymatic and non-enzymatic antioxidants, making cardiomyocytes more susceptible to reactive oxygen species.

On the other hand, there is a significant reduction in the MDA level associated with increased SOD, GPX, and GSH levels in the hearts of the ENC-DOX compared to animals administered DOX alone. The present findings are consistent with Awasthi *et al*. [49] the tumor's leaky vasculature, and improved retention and permeation of nanoparticles enable nanoparticles to localize intrinsically into tumor vessels resulting in sustained release of therapeutic drugs, the long half-life, high payloads, and subsequently reduce its toxicity on normal tissues. Also, Prokop [50] found that DOX-induced oxidative stress was antagonized by treatment with Doxorubicin loaded on pectin nanoparticles. This improvement in antioxidants may be due to the role of ENC-DOX. In addition, our study suggests that the improvement in antioxidants level may be due to the anti-lipid per-oxidative properties of ENC-DOX by its ability to scavenge free radical generation, which was evidenced by GSH and GPX elevation as well as SOD up-regulation.

In the contemporary study, implantation of EAC resulted in a significant increment in TNF-α and MCP-1 in heart tissue compared to the normal control group. This is significant because it causes pathological cardiac damage [51]. The current study's findings were in agreement with those of Abd El-Dayem *et al*. [52], who noted higher TNF- levels in female

mice with Ehrlich ascites cancer. The elevation in the level of the pro-inflammatory cytokine in EAC mice may be due to the increase in ROS production by macrophages, which stimulate lipid peroxidation [52].

Administration of free DOX resulted in a significant increase in cardiac TNF-α and MCP-1versus to EAC group. These results revealed the existence of inflammation in the heart of mice treated with DOX. Additionally, TNF- and interleukins are pro-inflammatory mediators that contribute to DOX-induced cardiotoxicity and cardiac hypertrophy by activating the p38 MAPK/NF-kB pathway [53]. These results agreed with Sirwi *et al*. [54], who stated that inflammation plays a key role in cardiotoxicity induced by Doxorubicin. Similarly, Benzer *et al*. [55] demonstrated that doxorubicin-induced cardiotoxicity is significantly mediated by pro-inflammatory cytokine production.

On the other hand, treatment with ENC-DOX caused a reduction in cardiac TNF-α and MCP-1 as compared to DOX group. These results are similar to Adeel *et al*. [56], who reported that nanoparticles have advantages over traditional chemotherapy, including reduced distribution in normal tissues and higher accumulation in tumors; the nanoparticles reduced toxicity, preventing adverse effects. In the view of our study, depletion of pro-inflammatory markers TNF-α and MCP-1 confirms the anti-inflammatory effect of ENC-DOX, and the scavenger capacity of free radicals of pectin extract was enhanced when encapsulated with Doxorubicin.

The present study showed an elevation in pro-apoptotic markers caspase-3 and P53 in heart tissue and a decrease in anti-apoptotic marker BCL2 in EAC group as compared to CON group. These results follow Yu *et al*. [48], who stated that if the damaged cells did not choose apoptosis, they could tend to turn into cancer. In view of our findings, Badr El-Din *et al*. [57] documented that in mice inoculated with Ehrlich ascites carcinoma, there are significant variations in the expression of apoptotic regulators (activation of caspase-3, up-regulation in the expression of pro-apoptotic proteins p53 and Bax, and down-regulation in the expression of the anti-apoptotic protein Bcl-2 and decreased Bcl2: Bax ratio). Also, the irregularity of anti-apoptotic Bcl2 family members is one of the identifying indicators of cancer cells compared to normal cells.

Treatment of EAC group with DOX was also up-regulating the heart caspase-3 and P53 correlated with down-regulating the cardiac level of Bcl-2 compared to the EAC group. Apoptosis and oxidative stress of cardiomyocytes are major mechanisms involved in DOX-induced cardiotoxicity [58]. Anti-apoptotic proteins like Bcl-2 are known to be depleted during the apoptosis process, while pro-apoptotic proteins like Bax and Caspase-3 are increased [59]. Our results also showed that in DOX-treated animals, expression of Bcl-2 decreased. Our finding is similar to Kluza *et al*. [60], who concluded that the extrinsic and intrinsic mitochondria-dependent apoptotic pathways could be triggered due to DOX-encouraged oxidative stress in cardiomyocytes. According to Deavall *et al*. [61] Bcl2 is an anti-apoptotic protein that inhibits apoptosis in cardiomyocytes by maintaining mitochondrial structure and function as well as preventing mitochondrial permeability transition. The buildup of p53 in the heart is crucial in doxorubicin-induced cardiomyocyte death [62]. Cory and Adams [63] explained that caspase activation leads to apoptosis through two main pathways in support of the current results. One pathway involves a tumor necrosis factor (TNF) receptor at the cell surface, which recruits caspase-8 through the adaptor protein FAS-associated death domain, leading to the activation of caspase-8.

In contrast, the treatment of the EAC group ENC-DOX recorded a significant reduction in the caspase-3 and p^{53} levels in the heart associated with a significant increment in the Bcl-2 level as compared to the DOX group. Our finding is in line with Krtaz [64], who claimed that the use of nanoparticles for a prolonged residence time of DOX was necessary due to the acidic functions in the ring phenolic groups of DOX and a basic function in the sugar amino group. This increased ability to co-deliver the drug to the target site and decreased systematic side effects.

According to these results, the anti-apoptotic effect of ENC-DOX is evidenced by elevation of BCL2 and depletion of caspase-3 in hepatocytes, confirming the treatment of Doxorubicin encapsulated within pectin nanoparticles can improve heart damage induced by DOX.

The present study demonstrated an increase in CK and LDH in the heart tissue of EAC-bearing mice versus the normal group. It is well-documented that cancer cells take most of the oxygen and nutrients from other normal cells. Our finding is inconsistent with Yu *et al*. [65], who stated that LDH and CK release from the heart and damage in the cell membrane of cardiac muscle is due to the deficiency of oxygen and nutrients to the myocardium. Thus, the elevated levels of these enzymes are considered biomarkers of cardiac damage.

EAC group treated with DOX showed a significant increase in the levels of CK and LDH in DOX group compared to EAC group. The elevated level of CK in doxorubicin-injected rats is suggestive of the deleterious effects of Doxorubicin on cardiomyocytes [66]. The heart is particularly vulnerable to ROS-induced injury due to its low antioxidant defenses and highly oxidative metabolism; therefore, an increase in CK and LDH concentration in the blood of animals receiving doxorubicin is anticipated [67].

Treatment with ENC-DOX resulted in marked improvement in the levels of CK and LDH as compared to treatment with free DOX. Our results are consistent with Peng *et al*. [68], who found that functional indexes of heart CK and LDH remained normal in the doxorubicin conjugated with pectin nanoparticles treated animals. Our results demonstrate that the treatment with ENC-DOX prevented LDH and CK elevation, which in turn repaired cardiac injury caused by DOX.

Histopathological examination of myocardium from the normal group revealed normal histology of the heart muscle fibers without any detectable alterations. On the other hand, the heart of EAC-bearing mice showed myocarditis manifested by intense mononuclear inflammatory cell infiltration between the muscle fibers. The muscle fibers suffered from vacuolar degeneration and necrosis. Pericarditis was noticed in some of the examined sections. The blood vessels within the myocardium were severely congested. In view of our finding, Ali *et al*. [69] reviewed that the proliferation and migration of tumor cells into the internal organs are thought to be responsible for the infiltrations of Ehrlich tumor cells, and the presence of Aggregations of inflammatory cells might occur to disorganization of the cytoplasm or degeneration of the mitochondria.

EAC group treated with DOX only showed mild degenerative changes in the myocardium. These results agree with Hassan *et al*. [70], who found that doxorubicin injection in rats resulted in cardiac muscle fibers degeneration, edema, and inflammatory cells. Ultrastructural studies also indicated degeneration of mitochondria and substantial loss of myofibrillar, which could result from free radical-mediated lipid peroxidation in the mitochondrial membrane.

On the other side, the heart section of the group that administrated ENC-DOX appeared nearly like the control, maintaining the normal cardiomyocyte's function, which indicates cardiac regeneration. Our findings may be due to the ability of nanoparticles to localize into tumor vessels and reduce the drug's toxicity to normal tissue.

4. Conclusions

Despite the broad spectrum of doxorubicin (DOX) as an anticancer agent, its clinical applications are limited owing to its-induced cardiotoxicity. Pectin nanoparticles PNPs are widely used in drug delivery systems and develop effective carriers for DOX. Encapsulation of Doxorubicin on Pectin nanoparticles improved DOX effect in all examined parameters of heart tissue in mice compared with DOX and tumor-bearing animals. This study proved that drug encapsulation on the pectin nanoparticles is safer than free DOX.

Funding

This research received no external funding.

Acknowledgments

Declared none.

Conflicts of Interest

The authors declare no conflict of interest.

References

1. Ferlay, J.; Colombet, M.; Soerjomataram, I.; Parkin, D.; Pineros, M.; Znaor, A. Cancer statistics for the year 2020: An overview. *International Journal of Cancer* **2021**, *149*, 778-789, https://doi.org/10.1002/ijc.33588.
2. Mutar, T.F.; Tousson, E.; Hafez, E.; Abo Gazia, M.; Salem, S.B. Ameliorative effects of vitamin b17 on the kidney against ehrlich ascites carcinoma induced renal toxicity in mice. *Environ. Toxicol.* **2020**, *35*, 528–537, https://doi.org/10.1002/tox.22888.
3. Dasari, S.; Njiki, S.; Mbemi, A.; Yedjou, C.G; Tchounwou, P.B. Pharmacological Effects of Cisplatin Combination with Natural Products in Cancer Chemotherapy. *International Journal of .Molecular Sciences* **2022**; *23*, https://doi.org/10.3390/ijms23031532.
4. Eisvand, F.; Imenshahidi, M.; Ghasemzadeh Rahbardar, M.; Tabatabaei Yazdi, S.A.; Rameshrad, M.; Razavi, B.M.; Hosseinzadeh, H. Cardioprotective effects of alpha-mangostin on doxorubicin-induced cardiotoxicity in rats. *Phytotherapy Research* **2022**, *36*, 506–524, https://doi.org/10.1002/ptr.7356.
5. Fang, H.; Wang, D.; Han, E.; Xie, X.; Yang, J.; Wei, S.; Gu, F.; Gao, N.; Zhu, X.; Yin, Q.; Cheng, P.; Zhang, W. Ferroptosis as target for protection against cardiomyopathy . *Proc. Natli. Acad. Sci. N. USA* **2019**, *116*, 2672-2680, https://doi.org/10.1073/pnas.1821022116.
6. Mohammed, H.S.; Hosny, E.N.; Khadrawy, Y.A.; Magdy, M.; Attia, Y.S.; Sayed, O.A.; AbdElaal, M. Protective effect of curcumin nanoparticles against cardiotoxicity induced by Doxorubicin in rat. *Biochimica ET Biophysica Acta (BBA)-Molecular Basis of Disease* **2020**, *1866*, https://doi.org/10.1016/j.bbadis.2020.165665.
7. Dupont, C.; Vandenplas, Y. Different thickening complexes with pectin in infant anti-regurgitation formula. *Acta Paediatr* **2020**, *109*, 471-480, https://doi.org/10.1111/apa.15015.
8. Deng, Y.; Zhang, X.; Shen, H.; He, Q.; Wu, Z.; Liao, W.; Yuan, M. Application of the Nano-Drug Delivery System in Treatment of Cardiovascular Diseases. *Front. Bioeng. Biotechnol.* **2020**, *7*, https://doi.org/10.3389/fbioe.2019.00489.
9. Tian, L.; Singh, A.; Singh, A.V. Synthesis and characterization of pectin-chitosan conjugate for biomedical application. *Int. J. Biol. Macromol.* **2020**, *153*, 533–538, https://doi.org/10.1016/j.ijbiomac.2020.02.313.
10. Wu, D.; Chen, S.; Ye, X.; Ahmadi, S.; Hu, W.; Yu, C.; He, Q. Protective effects of six different pectic polysaccharides on DSS-induced IBD in mice. *Food Hydrocolloids* **2021**, *127*, https://doi.org/10.1016/j.foodhyd.2021.107209.

11. Delphi, L.; Sepehri, H. Apple pectin: A natural source for cancer suppression in 4T1 breast cancer cells in vitro and express p53 in mouse bearing 4T1 cancer tumors, in vivo. *Biomed. Pharmacother* **2016**, *84*, https://doi.org/10.1016/j.biopha.2016.09.080.
12. Mahmoud, M.H.; Abou-Arab, A.A.; Abu-Salem, F.M. Effect of some different drying methods on the chemical analysis of citrus by-products. *Research Journal of Pharmaceutical Biological and Chemical Sciences* **2015,** *6*, 105-116.
13. Assadpour, E.; Jafari, S.M. Spray drying of folic acid within nanoemulsions: optimization by Taguchi approach. *Drying Technology* **2017**, *35*, 1152-1160, https://doi.org/10.1080/07373937.2016.1242016.
14. Mahmoud, M.H.; Mehaya, F.M.; Abu-Salem, F.M. Encapsulation Of Pomegranate Seed Oil Using W/O/W Nano-Emulsion Technique Followed By Spray Drying And Its Application In Jelly Form. *Journal of Microbiology, Biotechnology and Food Sciences* **2020**, *10*, 449-453, https://doi.org/10.15414/jmbfs.2020.10.3.449-453.
15. Hosseini S.F.; Rezaei, M.; Zandi, M.; Farahmandghavi, F. Fabrication of bio-nanocomposite films based on fish gelatin reinforced with chitosan nanoparticles. *Food hydrocolloids* **2015**, *44*, 172-182, https://doi.org/10.1016/j.foodhyd.2014.09.004.
16. Vincent, P.C.; Nicholls, A. Comparison of the growth of the Ehrlich Ascites Tumor in male and female mice. *Cancer Res* **1967**, *27*, 1058-1065.
17. Khedr, N.F.; Khalil, R.M. effect of hesperidin on mice bearing earlish solid carcinoma maintained in Doxorubicin. *Tumor boil* **2015**, *36*, 9267-9275, https://doi.org/10.1007/s13277-015-3655-0.
18. Strober, W. Trypan blue exclusion test of cell viability. *Curr Protoc Immunol* **2001**, *21*, 1-2, https://doi.org/10.1002/0471142735.ima03bs111.
19. Perry, M.J. *The chemotherapy source book.* Wolters Kluwer Health/lippincott Williams and Wilkins **2008**, Philadelphia
20. Verma, K.; Leekha, A.; Kumar, V.; Moin, I.; Kumar, S. Biodistribution and In-vivo Efficacy of Doxorubicin Loaded Chitosan Nanoparticles in Ehrlich Ascites Carcinoma (EAC) Bearing Balb/c Mice. *J Nanomed Nanotechnol* **2018**, *9*, https://doi.org/10.4172/2157-7439.1000510.
21. Li, Z.P.; Jiang, M.C.; Chen, B.; Gao, P.; Yang, S.; Liu, Y.F.; Ye, P.J.; He, D.X.; Huang, H.L.; Yu, C.Y. Fabrication and characterization of a novel self-assembling micelle based on chitosan cross-linked pectin-doxorubicin conjugates macromolecular pro-drug for targeted cancer therapy. *RSC Adv* **2018**, *8*, 12004-12016, https://doi.org/10.1039/C8RA01403E.
22. Fahim, A.Y.; Esmat, E.A.; Mady, E.K. Ibrahim, Antitumor activities of Iodo acetate and Di methyl sulphoxide against solid Ehrlich carcinoma growth in mice. *Biol Res* **2003**, *36*, 253-62, http://dx.doi.org/10.4067/S0716-97602003000200015.
23. Ohkawa, H.; Ohishi, W.; Yagi, K. Assay for lipid peroxidase in animal tissue by thiobarbituric acid reaction. *Anal. Biochem* **1979**, *95*, 351-358, https://doi.org/10.1016/0003-2697(79)90738-3.
24. Nishikimi, M.; Roa, N.A.; Yogi, K. Colorimetric determination of superoxide dismutase. *Biochem. Bioph. Common* **1972**, *46*, 849-854.
25. Beutler, E.; Duron, O.; Kelly, B.M. Improved Method for the Determination of Blood Glutathione. *Journal of Laboratory and Clinical Medicine* **1963**, *61*, 882-888.
26. Paglia, D.E.; Valentine, W.N. Studies on the Quantitative and Qualitative Characterization of Erythrocyte Glutathione Peroxidase. *Journal of Laboratory and Clinical Medicine* **1967**, *70*, 158-169.
27. Banchroft, J.D.; Stevens, A.; Turner, D.R. *Theory and practice of histological techniques.* 4th ed. New York, London, San Francisco, Tokyo: Churchil Livingstone. **1996;** https://doi.org/10.1111/j.1365-2559.1990.tb00755.x.
28. Ilyasogluand, H.; El, S.N. Nanoencapsulation of EPA/DHA with sodium caseinate–gum arabic complex and its usage in the enrichment of fruit juice. *LWT-Food Science and Technology* **2014**, *56*, 461-468, https://doi.org/10.1016/j.lwt.2013.12.002.
29. Prichapan, N.; Klinkesorn, U. Factor affecting the properties of water-in-oil-in-water emulsions for encapsulation of minerals and vitamins. *Songklanakarin Journal of Science & Technology* **2014**, *36*, 651–661.
30. Buyukkestelli, H.I.; El, S.N. Development and characterization of double emulsion to encapsulate iron. *Journal of Food Engineering* **2019**, *263*, 446-453, https://doi.org/10.1016/j.jfoodeng.2019.07.026.
31. Dasgupta, N.; Ranjan, S.; Mundra, S.; Ramalingam, C.; Kumar, A. Fabrication of food grade vitamin E nanoemulsion by low energy approach, characterization and its application. *Int J Food Prop* **2016**, *19*, 700–708, https://doi.org/10.1080/10942912.2015.1042587.
32. Khazaei, K.M.; Jafari, S.M.; Ghorbani, M.; Kakhki, A.H. Application of maltodextrin and gum Arabic in microencapsulation of saffron 'petal's anthocyanins and evaluating their storage stability and color. *Carbohydrate polymers* **2014**, *105*, 57-62, https://doi.org/10.1016/j.carbpol.2014.01.042.
33. Jafari, S.M.; He, Y.; Bhandari, B. Encapsulation of nanoparticles of d-limonene by spray drying: role of emulsifiers and emulsifying techniques. *Drying Technology* **2007,** *25*, 1069-1079, https://doi.org/10.1080/07373930701396758.
34. Mahdavee Khazaei, K.; Jafari, S.M.; Ghorbani, M.; Hemmati, K. Optimization of anthocyanin extraction in 'Saffron's petal with response surface methodology. *Research and Innovation in Food Science and Technology* **2014**, *3*, 37-50, https://doi.org/10.1007/s12161-015-0375-4.

35. Tamjidi, F.; Shahedi, M.; Varshosaz, J.; Nasirpour, A. Design and characterization of astaxanthin-loaded nanostructured lipid carriers. *Innovative Food Science & Emerging Technologies* **2014**, *26*, 366-374, https://doi.org/10.1016/J.IFSET.2014.06.012.
36. Guo, X.; Zhao, W.; Pang, X.; Liao, X.; Hu, X.; Wu, J. Emulsion stabilizing properties of pectins extracted by high hydrostatic pressure, high-speed shearing homogenization and traditional thermal methods: A comparative study. *Food Hydrocolloids* **2014**, *35*, 217-225, https://doi.org/10.1016/j.foodhyd.2013.05.010.
37. Lara-Espinoza, C.; Carvajal-Millan, E.; Balandran-Quintana, R.; Lopez-Franco, Y.; Rascon-Chu, A. Pectin and Pectin-Based Composite Materials: Beyond Food Texture. *Molecules* **2018**, *23*, https://doi.org/10.3390/molecules23040942.
38. Wang, Y.; Liu, S.; Tian, Y.; Wang, Y.; Zhang, Q.; Zhou, X.; Meng, X. N. Song, Prognostic role of galectin-3 expression in patients with solid tumors: A meta-analysis of 36 eligible studies. *Cancer Cell Int* **2018**, *18*, https://doi.org/10.1186/s12935-018-0668-y.
39. Sayed, A.; Munir, M.; Nabet, M.S.; Alghamdi, B.S.; Ashraf, G.M.; Bahbah, E.I.; Elfil, M. Galectin-3: A Novel Marker for the Prediction of Stroke Incidence and Clinical Prognosis. *Mediators of Inflammation* **2022**, *2022*, https://doi.org/10.1155/2022/2924773.
40. Matarrese, P.; Tinari, N.; Semeraro, M.L.; Natoli, C.; Iacobelli, S.; Malorni, W. Galectin-3 overexpression protects from cell damage and death by influencing mitochondrial homeostasis. *FEBS Letter* **2000**, *473*, 311-315, https://doi.org/10.1016/S0014-5793(00)01547-7.
41. Gao, X.; Zhi, Y.; Zhang, T.; Xue, H.; Wang, X.; Foday, A.D. Analysis of the neutral polysaccharide fraction of MCP and its inhibitory activity on galectin-3. *Glycoconjugate Journal* **2012**, *29*, 159-165, https://doi.org/10.1007/s10719-012-9382-5.
42. Zhang, Y.; Sun, T.; Jiang, C. Biomacromolecules as carriers in drug delivery and tissue engineering. *Acta Pharm Sin B* **2018**, *8*, 34-50, https://doi.org/10.1016/j.apsb.2017.11.005.
43. Naqash, F.; Masoodi, F.A.; Rather, S.A.; Wani, S.M.; Gani, A. Emerging concepts in the nutraceutical and functional properties of pectin-A Review. *Carbohydr Polym* **2017**, *168*, 227-239, https://doi.org/10.1016/j.carbpol.2017.03.058.
44. Whitby, L.; Smith, A.; Backett, G.; Walker, S. *Lecture Notes in Clinical Biochemistry*. 5th ed. Oxford: Blackwell Scientific Publishers **1993**; pp. 105–123, https://doi.org/10.1016/0307-4412(94)90071-X.
45. Forman, H.J.; Zhang, H. Targeting oxidative stress in disease: Promise and limitations of antioxidant therapy. *Nat Rev Drug Discov* **2021**, *20*, 689–709, https://doi.org/10.1038/s41573-021-00233-1.
46. Sun, J.; Sun, G.; Cui, X.; Meng, X.; Qin, M.; Sun, X. Myricitrin protects against doxorubicin-induced cardiotoxicity by counteracting oxidative stress and inhibiting mitochondrial apoptosis via ERK/P53 pathway. *Evidence-based Complementary and Alternative Medicine* **2016**, *2016*, https://doi.org/10.1155/2016/6093783.
47. Abd El-Dayem, S.M.; Fouda, F.; Helal, M.; Zaazaa, A. The role of Catechin against doxorubicin-induced cardiotoxicity in Ehrlich ascites carcinoma cells (EAC) bearing mice. *American Journal of Science* **2010**, *6*, 146–152.
48. Yu, X.; Cui, L.; Zhang, Z.; Zhao, Q.; Li, S. α-Linolenic acid attenuates doxorubicininduced cardiotoxicity in rats through suppression of oxidative stress and apoptosis. *Acta Biochim. Biophys Sin* **2013**, *45*, 817–826.
49. Awasthi, R.; Roseblade, A.; Hansbro, P.M. Nanoparticles in cancer treatment: opportunities and obstacles. *Curr Drug Targets* **2018**, *19*, 1696-1709, https://doi.org/10.2174/1389450119666180326122831.
50. Prokop, A.; Davidson, J.M. Nanovehicular intracellular delivery systems. *J Pharm Sci* **2008**, *97*, 3518-90, https://doi.org/10.1002/jps.21270.
51. Hoek, J.B.; Pastorino, J.G. Ethanol, oxidative stress, and cytokine-induced liver cell injury. *Alcohol* **2002**, *27*, 63–68, https://doi.org/10.1016/S0741-8329(02)00215-X.
52. Abd El-Dayem, S.M.; Fouda, F.M.; Ali, E.H.; Abd El Motelp, B.A.The antitumor effects of tetrodotoxin and/or Doxorubicin on Ehrlich ascites carcinoma-bearing female mice. *Toxicology and Industrial Health* **2012**, *29*, 404–417, https://doi.org/10.1177/0748233711434955.
53. Guo, R.M.; Xu, W.M.; Lin, J.C. Activation of the p38 MAPK/NF-kappaB pathway contributes to doxorubicin-induced inflammation and cytotoxicity in H9c2 cardiac cells. *Mol Med Rep* **2013**, *8*, 603–608, https://doi.org/10.3892/mmr.2013.1554.
54. Sirwi, A.; Shaik, R.A.; Alamoudi, A.J.; Eid, B.G.; Elfaky, M.A.; Ibrahim, S.R.M.; Mohamed, G.A.; Abdallah, H.M.; Abdel-Naim, A.B. Mokko Lactone Alleviates Doxorubicin-Induced Cardiotoxicity in Rats via Antioxidant, Anti-Inflammatory, and Antiapoptotic Activities. *Nutrients* **2022**, *14*, https://doi.org/10.3390/nu14040733.
55. Benzer, F.; Kandemir, F.M.; Ozkaraca, M; Kucukler, S.; Caglayan, C. Curcumin ameliorates doxorubicin-induced cardiotoxicity by abrogation of inflammation, apoptosis, oxidative DNA damage, and protein oxidation in rats. *J. Biochem. Mol. Toxicol* **2018**, *32*, https://doi.org/10.1002/jbt.22030.
56. Adeel, M.; Duzagac, F.; Canzonieri, V.; Rizzolio, F. Self-Therapeutic Nanomaterials for Cancer Therapy: A Review. *ACS Appl. Nano Mater* **2020**, *3*, 4962–4971, https://doi.org/10.1021/acsanm.0c00762.
57. Badr El-Din, N.K.; Ali, D.A.; Abou-El-Magd, R.F. Grape seeds and skin induce tumor growth inhibition via G1-phase arrest and apoptosis in mice inoculated with Ehrlich ascites carcinoma. *Nutrition Journal* **2019**, *58*, 100-9, https://doi.org/10.1016/j.nut.2018.06.018.

58. Asensio-Lopez, M.C.; Soler, F.; Pascual-Figal, D. Doxorubicin-induced oxidative stress: the protective effect of nicorandil on HL-1 cardiomyocytes. *PLoS One* **2017**, *12*, https://doi.org/10.1371/journal.pone.0172803.
59. Sahu, B.D.; Kumar, J.M.; Kuncha, M.; Borkar, R.M.; Srinivas, R.; Sistla, R. Baicalein alleviates doxorubicin-induced cardiotoxicity via suppression of myocardial oxidative stress and apoptosis in mice. *Life Sci* **2016**, *144*, 8–18, https://doi.org/10.1016/j.lfs.2015.11.018.
60. Kluza, J.; Marchetti, P.; Gallego, M.A.; Lancel, S.; Fournier, C.; Loyens, A.; Beauvillain, J.C.; Bailly, C. Mitochondrial proliferation during apoptosis induced by anticancer agents: effects of Doxorubicin and mitoxantrone on cancer and cardiac cells. *Oncogene* **2004**, *23*, 7018–7030, https://doi.org/10.1038/sj.onc.1207936.
61. Deavall, D.G.; Martin, E.A.; Horner, J.M.; Roberts, R. Drug-induced oxidative stress and toxicity. *J Toxicol* **2012,** *2012*, 645-460, https://doi.org/10.1155/2012/645460.
62. Zhu, W.; Soonpaa, M.H.; Chen, H.; Shen, W.; Payne, R.M.; Liechty, E.A.; Caldwell, R.L.; Shou, W.; Field, L.J. Acute doxorubicin cardiotoxicity is associated with p53- induced inhibition of the mammalian target of rapamycin pathway. *Circulation* **2009**, *119*, 99–106, https://doi.org/10.1161/CIRCULATIONAHA.108.799700.
63. Cory. S.; Adams, J.M. The BCL family: regulators of the cellular life-or-death- switch. *Cancer Nature Reviews* **2002**, *2*, 647–656, https://doi.org/10.1038/nrc883.
64. Kratz, F. Albumin as a drug carrier: design of prodrugs, drug conjugates and nanoparticles. *J Control Release* **2008**, *132*, 171-183, https://doi.org/10.1016/j.jconrel.2008.05.010.
65. Yu, W.; Sun, H.; Zha, W.; Cui, W.; Xu, L.; Min, Q.; Wu, J. Apigenin attenuates adriamycin-induced cardiomyocyte apoptosis via the PI3K/AKT/mTOR pathway. *Evidence-based Complementary and Alternative Medicine* **2017**, *2017*, https://doi.org/10.1155/2017/2590676.
66. Nagoor Meeran, M.F.; Jagadeesh, G.S.; Selvaraj, P. Thymol attenuates inflammation in isoproterenol induced myocardial infarcted rats by inhibiting the release of lysosomal enzymes and downregulating the expressions of pro-inflammatory cytokine. *Eur. J. Pharmacol* **2015**, *754*, 153–161, https://doi.org/10.1016/j.ejphar.2015.02.028.
67. Injac, R.; Perse, M.; Cerne, M.; Potocnik, N.; Radic, N.; Govedarica, B.; Djordjevic, A.; Cerar, A.; Strukelj, B. Protective effects of fullerenol C60(OH)24 against doxorubicin-induced cardiotoxicity and hepatotoxicity in rats with colorectal cancer. *Biomaterials* **2009**, *30*, 1184-1196, https://doi.org/10.1016/j.biomaterials.2008.10.060.
68. Ye, P.J.; Huang, C.; Yang, S.; Gao, P.; Li, Z.P.; Tang, S.Y.; Xiang, Y.; Liu, Y.F.; Chen, Y.P.; He, D.X.; Yu, C.Y. Facile fabrication of a novel hybrid nanoparticles by self-assembling based on pectin-doxorubicin conjugates for hepatocellular carcinoma therapy. *Artif Cells Nanomed Biotechnol* **2018**, *46*, S661-S670, https://doi.org/10.1080/21691401.2018.1505745.
69. Ali, D.A.; Badr El-Din, N.K.; Abou-El-Magd, R.F. Antioxidant and hepatoprotective activities of grape seeds and skin against Ehrlich solid tumor induced oxidative stress in mice. *Egyptian Journal of Basic and Applied Sciences* **2015**, *2*, 98-109, https://doi.org/10.1016/j.ejbas.2015.02.003.
70. Al-Taee, H.; Azimullah, S.; Meeran, M.F.N.; Alaraj Almheiri, M.K.; Al Jasmi, R.A.; Tariq, S.; Ab Khan, M.; Adeghate, E.; Ojha, S. β-caryophyllene, a dietary phytocannabinoid attenuates oxidative stress, inflammation, apoptosis and prevents structural alterations of the myocardium against doxorubicin-induced acute cardiotoxicity in rats: An in vitro and in vivo study. *European Journal of Pharmacology* **2019**, *858*, https://doi.org/10.1016/j.ejphar.2019.172467.